Resolving the missing link between single platelet force and clot contractile force

Yueyi Sun¹, Oluwamayokun Oshinowo^{2,3,4,5,6}, David R. Myers^{2,3,5,6}, Wilbur A. Lam^{2,3,4,5,6}, & Alexander Alexeev¹

SUMMARY

Blood clot contraction plays an important role in wound healing and hemostasis. While clot contraction is known to be driven by platelets that extend and retract filopodia to apply contraction force to the neighboring fibrin fibers, how single platelet forces relate to the forces generated by macroscopic clots remains largely unknown. Using our microfabricated high-throughput platelet contraction cytometer, we find that single platelets have an average force of 34 nN (n = 10 healthy individuals), with a range of 0 – 100 nN in microenvironmental conditions known to maximize platelet force within a clot. However, multiple bulk clot experimental systems predict a normalized single platelet mean force lower than 0.5 nN. To resolve this discrepancy, we use a mesoscale computational model informed by our experimental measurements to probe the mechanism by which individual platelets induce forces in macroscopic clots. Our experimentally informed model shows that number of platelets in the clot cross section defines the net clot force. For ease, we provide an intuitive relationship resolving single platelet force and the clot force, and demonstrate that this relationship is applicable to a variety of physiologically relevant clot configurations and attachment conditions. The correlation between the microscale platelet biophysical properties and the macroscale behavior of the clot is useful to better understand blood disorders associated with bleeding and thrombosis, and facilitates the development of platelet-based and platelet-mimetic biomaterials.

¹ George W. Woodruff School of Mechanical Engineering, Georgia Institute of Technology, 801 Ferst Drive, Atlanta, GA 30332-0405, USA

² Department of Pediatrics, Division of Pediatric Hematology/Oncology, Aflac Cancer Center and Blood Disorders Service of Children's Healthcare of Atlanta, Emory University School of Medicine, Atlanta, GA 30322.

³ The Wallace H. Coulter Department of Biomedical Engineering, Georgia Institute of Technology & Emory University, Atlanta, GA, 30332.

⁴ Winship Cancer Institute of Emory University, Atlanta, GA, 30322.

⁵ Parker H. Petit Institute of Bioengineering and Bioscience, Georgia Institute of Technology, Atlanta, GA 30332.

⁶ Institute for Electronics and Nanotechnology, Georgia Institute of Technology, Atlanta, GA 30332.

INTRODUCTION

Platelets play a critical role in blood clotting and wound healing. At vascular injury sites, a cascade of signaling events leads to the formation of a soft platelet-fibrin clot which then retracts to restore normal blood flow [1]. The clot retraction is driven by platelets actively apply contraction forces to pull in the surrounding nascent fibrin fibers. The contraction force is generated by the retraction of filopodia [2], leading to a gradual decrease of the clot size and an increase of the clot mechanical stiffness [3-5]. Blood clot mechanical properties, such as the bulk modulus and the generated contractile forces, are correlated with the ability of platelets to contract fibrin network [5]. Despite the fact that platelets are the drivers of clot contraction and that resulted clot mechanics manifests itself in blood bleeding and clotting disorders [5-8], stroke [9], coronary artery disease [10], asthma [11, 12] and other pathologies [13, 14], how platelets work together to drive the macroscale clot contraction and what relationship exists between single platelet forces and the emerging clot force are still open questions. While single platelets have been experimentally shown to contract with forces up to 100 nN [3, 5, 7, 15], the average platelet forces evaluated using bulk clot force measurements are significantly lower [15]. Dividing the experimentally measured bulk clot force by the number of platelets yields single platelet forces lower than 1 nN [4, 5, 15-17].

Platelet-fibrin systems find increasing number of applications in novel biomaterials. When a normal blood flow is restored after the injury, the contracted platelet-fibrin clots act to stabilize wound fields, reattach tissue, protect the wound sites from external infections, release various growth factors and matrix remodeling enzymes, and support migration of cells for the tissue regeneration during the complex wound healing process [18, 19]. These diverse functions attributed to platelet-fibrin clots motivated researchers to focus on the development and clinical applications of platelet based biomaterials, such as platelet gel, platelet rich plasma (PRP), platelet fibrin glue (PFG), and platelet rich fibrin (PRF) [20-24]. Studies show that platelet derived biomaterials can be applied as effective sealing agents to reduce blood loss in surgeries [25], promote regeneration of tissue and bone [26], have significant potential for closing of

nonhealing venous ulcers [27], and can be used to induce nerve recovery across wide gaps [28]. Although these platelet derived biomaterials vary in preparation procedure, composition and application [21], they all rely on the clot formation and contraction processes, leading to the formation of a graft or membrane that is applied to a treated wound site. It has been reported that the mechanical strength and adhesive properties of the platelet-fibrin grafts and membranes affect cellular behaviors including cell migration and proliferation [29, 30]. Furthermore, clot mechanics affects how well the biomaterial can be molded to fit the wound site and defines the stability of the graft against unpredictable resorption [31], which are critical factors of successful wound healing treatments. One of the challenges in developing PRF and PGF is that the preparation procedure leads to limited volume of the material due to the clot contraction. More generally, the preparation and composition of platelet-derived biomaterials leading to the optimal therapeutic efficiency are open questions [21]. There is also a rising interest in designing semisynthetic and fully synthetic platelets that can be integrated with biomaterials to improve wound healing outcomes [32]. Thus, better understanding of the physical mechanisms by which platelets contract fibrin network and how single platelet forces relate to the clot forces and material properties are needed to facilitate the future development and application of novel platelet-derived biomaterials.

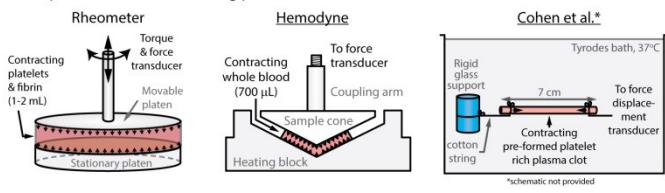
Historically, two main approaches were used to evaluate the platelet contractile force. Some researchers performed force measurements of bulk clots contracting between two parallel surfaces (Figure 1a), and then calculated the contractile force per platelet by averaging the measured clot force to the number of platelets within the clot (Figure 1b) [4, 5, 16, 17]. The magnitude of the contractile force per platelet varies greatly from an experiment to experiment. In Cohen's experiments with clots inside siliconized glass tubes [17] this force is about 0.012 nN, whereas in the rheometer and hemodyne experiments [4, 5, 16] it is in the range 0.4 - 0.51 nN (Figure 1b).

With the advent of new technologies, it has become possible to directly measure single platelet forces. Our system, the platelet contraction cytometer (Figure 1c), measures single platelet force in high-throughput and allows for complete control of the mechanical and biochemical microenvironments [5, 33].

In our system, thousands of fibrinogen microdot pairs are micropatterned on a flexible polyacrylamide hydrogel surface. Platelets adhere to single microdots, spread to neighboring microdots and contract, pulling these microdots closer together. Because of the high fidelity of our microfabricated system, only a single fluorescent image is necessary to calculate force, as contraction force is directly proportional to the microdot displacement. Here, we provide data on measurements of platelets from 10 healthy donors and show that single platelets apply forces between 1 nN and 100 nN, with an average force of about 34 nN (Figure 1c). Thus, our more comprehensive data set broadly agrees with single platelet forces measured in other experiments [3, 7, 15].

While both the contractile force per platelet measured by bulk clot contraction and the single platelet force measurements describe platelet force during contraction, and each can be used as a clinical measure of platelet function linked to different diseases [5, 7, 8, 34], there are 2 to 4 orders of magnitude differences between their values. The inconsistency noticed by Henriques et. al. [15] was attributed to the complex platelet interaction causing the platelet forces to not add up linearly in clots. Although studies have been done to better understand the single platelet behavior driving the clot contraction [2, 3, 5, 35] and the role of platelets heterogeneity enhancing the platelet contraction efficiency [36], there is currently no experimental tool capable of monitoring the generation and transmission of forces on the single platelet level within a contracting clot. Here, we employ a mesoscale computational model to simulate the clot contraction process under physiological conditions [36]. The model predicts the clot force based on the activity of individual platelets applying forces to the surrounding fibrin filaments (Figure. 1d). The model allows us to closely examine the evolution of forces generated by individual platelets as they contract within a clot and evaluate the emerging clot force. Our model explicitly accounts for the properties of the fibrin mesh and platelets, including their heterogeneity, and properly captures the mechanics of clot contraction [36]. Using this model we demonstrated that intrinsic platelet heterogeneity leading to asynchrono-mechanical amplification plays a critical role in efficient clot contraction [36].

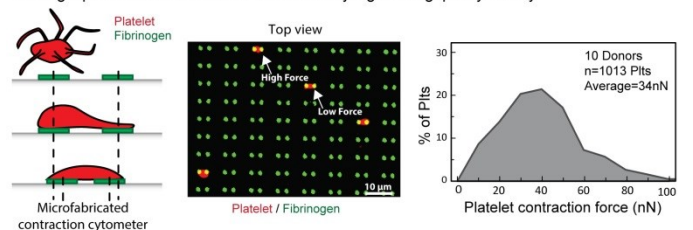
a. Experimental tools measuring platelet contractile forces



b. Contractile force per platelet calculated from experimental clot force measurements

Tool Author	Rheometer		Hemodyne	Isometric
	Jen	Myers	Carr	Cohen
Platelet concentration (plt/mL)	3x10 ⁸	2.5x10 ⁸	2.5x10 ⁸	3.3x10 ⁸
Clot volume (mL)	2.0	1.5	0.7	0.9
Cross-section area (m^2)	2.5x10 ⁻³	2x10 ⁻³	9x10 ⁻⁴	2x10 ⁻⁵
Clot height (µm)	800	750	780	45837
Clot force (N)	2.9x10 ⁻¹	1.9x10 ⁻¹	7.4x10 ⁻²	3.5x10 ⁻³
Clot stress (N/m^2)	116	95	82	176
Contractile force per platlet (nN)	0.49	0.51	0.40	0.012

c. Single platelet contractile forces measured by high-throughput cytometry



d. Simulated clots contracting between walls reproduce the dynamics of clot force generation measured in experiments

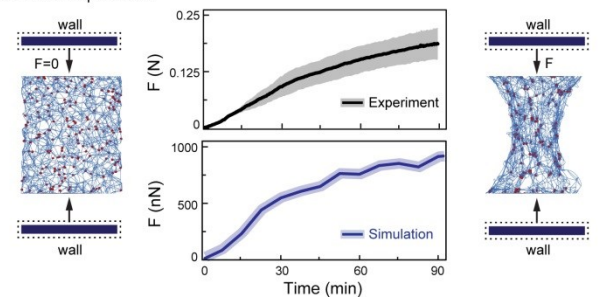


Figure 1: (a) Various experimental setups for measuring bulk clot contractile forces all of which may be used to derive contractile force per platelet. Left: rheometers suspend platelet and fibrin clots between plates and measure forces along with clot viscoelastic properties. Middle: hemodyne system measure whole blood clot contraction in a similar manner to the rheometer, although it is more streamlined for clinical use. Right: Cohen's measurement [17] are preformed after cold liquid is used to temporarily halt contraction while tying the clot to a support and transducer with cotton string (b) The contractile clot force per platelet calculated based on the experimental bulk clot force measurements in (a) vary from 0.012 nN to 0.51 nN. (c) High-throughput microfabricated contraction cytometers are used here to measure single platelet forces. Left: Fibrinogen microdot pairs are covalently bound to a deformable polyacrylamide hydrogel of known mechanical properties, as a platelet adheres and pulls pairs of microdots together, the contractile force is proportional to the microdot displacement. Middle: a confocal image showing single platelets (red) contracting against fibrinogen microdot pairs (green) on the hydrogel surface. Right: histogram of measured single platelet forces from 10 healthy individuals (n = 1013 platelets). (d) A simulated platelet-fibrin clot contracts between two parallel rigid walls, from the initial uncontracted state at t = 0 to the final contracted state at t = 90 minutes. The simulated clot applies an increasing force F on the walls, as more platelets are activated over time. The force reaches the maximum at the end of the contraction period, showing the same behavior as the experimentally measured clot force. Simulated platelets are shown in red and fibrin fibers are in blue.

RESULTS AND DISCUSSION

In our simulation, we place initial platelet-fibrin clots with cross-sectional area A, height H, and volume V = AH, sandwiched between two rigid walls (Figure. 1d). The clot is constructed from randomly oriented interconnected fibers and is populated with N = nV randomly distributed platelets, where n is the platelet count per unit volume. Our model incorporates platelet biophysical heterogeneity leading to asynchronous contraction onset within platelet population and asynchronous filopodia retraction by individual platelets [36]. Contraction of the clots starts at time t = 0 as a portion of platelets is activated, whereas other platelets remain at rest. The remaining platelets are sequentially activated during the 90 minute clot contraction period. Once a platelet is activated, it extends up to 12 filopodia in 3 successive waves that randomly grab and pull surrounding fibrin fibers, with each filopod pulls with a force that does not exceed 10 nN (Figure 2a: i). Each platelet is active for approximately 20 minutes. Since platelets are suspended in the fibrin mesh, the effective force imposed by a platelet on the surrounding fibrin fibers is $0 < f_s < 60$ nN depending on the extension and distribution of the filopodia (Figure 2a: ii-iv). This force range agrees with experimental measurements of single platelet forces [3, 5, 15]. To simulate the clot contraction dynamics, platelets are sequentially activated at different times throughout the clot contraction period to mimic platelet heterogeneity in blood clotting [36].

As the clot contracts, the clot force F applied to the wall steadily increases, consistently with the experimentally measured clot force (Figure 1c). We find that for a given platelet concentration, clots with different cross-sectional geometries, volumes (V = AH), and aspect ratios (Ar = H/ \sqrt{A}) generate similar magnitudes of the normal wall stress σ = F/A at the end of the contraction. This indicates that the clot force is proportional to the clot cross-sectional area and is independent from the clot height (Figure 2b) and the cross-sectional shape (Figure 2c and Supplementary Figure 1).

The force F is a result of the platelet collective pulling of the fibrin mesh. Within a contracting clot, the local forces applied by active platelets vary among the platelets within the clot. As more platelets

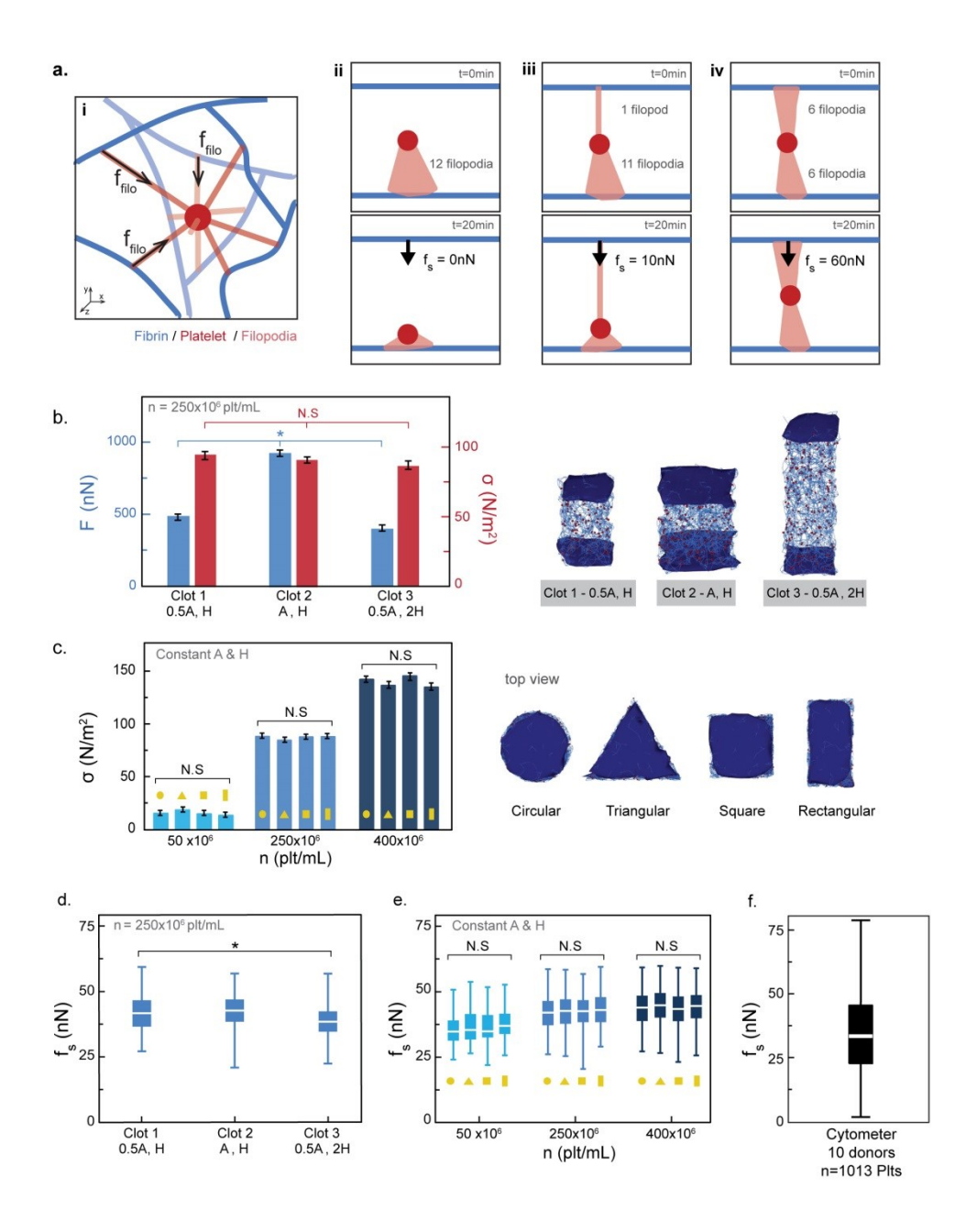


Figure 2: (a) A model platelet (in red) contracts surrounding fibrin fibers (in blue) through the extension and retraction of filopodia (in pink) (i). When a platelet is suspended between two fibrin fibers, the effective force f_s applied locally by this platelet can range between 0 to 60 nN, depending on how the filopodia are distributed (ii-iv). (b) Simulated platelet-fibrin clots 1, 2 and 3 with different combinations of A and H apply significantly different F (P < 0.05) but the same stress σ (P > 0.05) to the walls (in dark blue). The clots have constant platelet count per unit volume $n = 250 \times 10^6$ plt/mL and volume V. (c) At fixed n, the cross-section shapes of simulated platelet-fibrin clots (circular, triangular, square, rectangular) do not affect F and σ applied to the walls, P > 0.05 among the clots with same n.(d) The platelets within simulated clots 1, 2 and 3 in (b) generate similar local single platelet forces f_s with a consistent mean value. Although statistical testing shows a significant difference between clot 1 and clot 3 (P < 0.05), the biological relevance of this small difference is unclear. (e) Platelets apply consistent local single platelet forces f_s in clots with different cross-sectional geometries, P > 0.05 among the clots with same n. (f) Distribution of f_s in the experimental microfabricated contraction cytometer using 1013 platelets from 10 healthy donors. From (d) to (f), the boxes denote the median and quartiles, the top and bottom lines denote the maximum and minimum values, excluding the outliers.

complete contraction, the average of f_s steadily increases and reaches the maximum at t=90 minutes (Supplementary Figure 2 and Supplementary Video 1). In a fully contracted clot, f_s applied by individual platelets is distributed between 20 nN to 60 nN with an average around 40 nN (Figure 2d and 2e), matching with the experimental contraction cytometry measurements where 80% of platelets contracted with a force between 20 nN and 60 nN with an average force of 34 nN (Figure 2f). This force distribution is similar for clots with different cross-sectional geometries and combinations of A and H, indicating that the force applied by individual platelets is independent from these factors (Figure 2d, 2e and Supplementary Figure 3).

To explain how F changes depending on the clot cross-sectional geometry, size, and aspect ratio, we assume simplified clot configurations where each platelet applies an equal amount of force f. When contracting platelets are arranged in parallel between two surfaces, the force $F = N_1 f$, where N_1 is the number of platelets in the layer. When, on the other hand, the platelets are arranged in series, the force on the walls is limited by the single platelet force F = f (Figure 3a). Thus, the number of platelets working in parallel in a clot determines the overall clot force. To estimate the number of platelets that contract in parallel in a clot where platelets are randomly distributed, we assume that the average distance between any adjacent platelets is $d = n^{-1/3}$ (Figure 3b). Further assuming that the platelet layer thickness is d, we estimate the number of platelets in a layer parallel to the wall is equal to $N_1 = N/(H/d) = n^{2/3}A$ (Figure 3c). Thus, the clot force is related to the single platelet force by $F = fN_1 = fn^{2/3}A$.

The above relationship can be used to evaluate the mean platelet force within a clot based on the net force exerted by the clot as $f_c = F/(n^{2/3}A)$, thereby directly connecting the single platelet force and clot force. We find that the clot forces measured in experiments [4, 5, 16, 17] yield f_c with similar values that are also close to the average of experimentally measured single platelet force f_s [3, 5, 15] (Figure 3d). When compared to our simulation results, we find close agreement with the experimental values when f_c is calculated using the simulated clot force. On the other hand, when we calculate f_s directly using the

forces exerted by platelets within simulated clots, we find that in this case the average of f_s exceeds the experimental values. We related this difference to the fact that individual platelets apply force in all

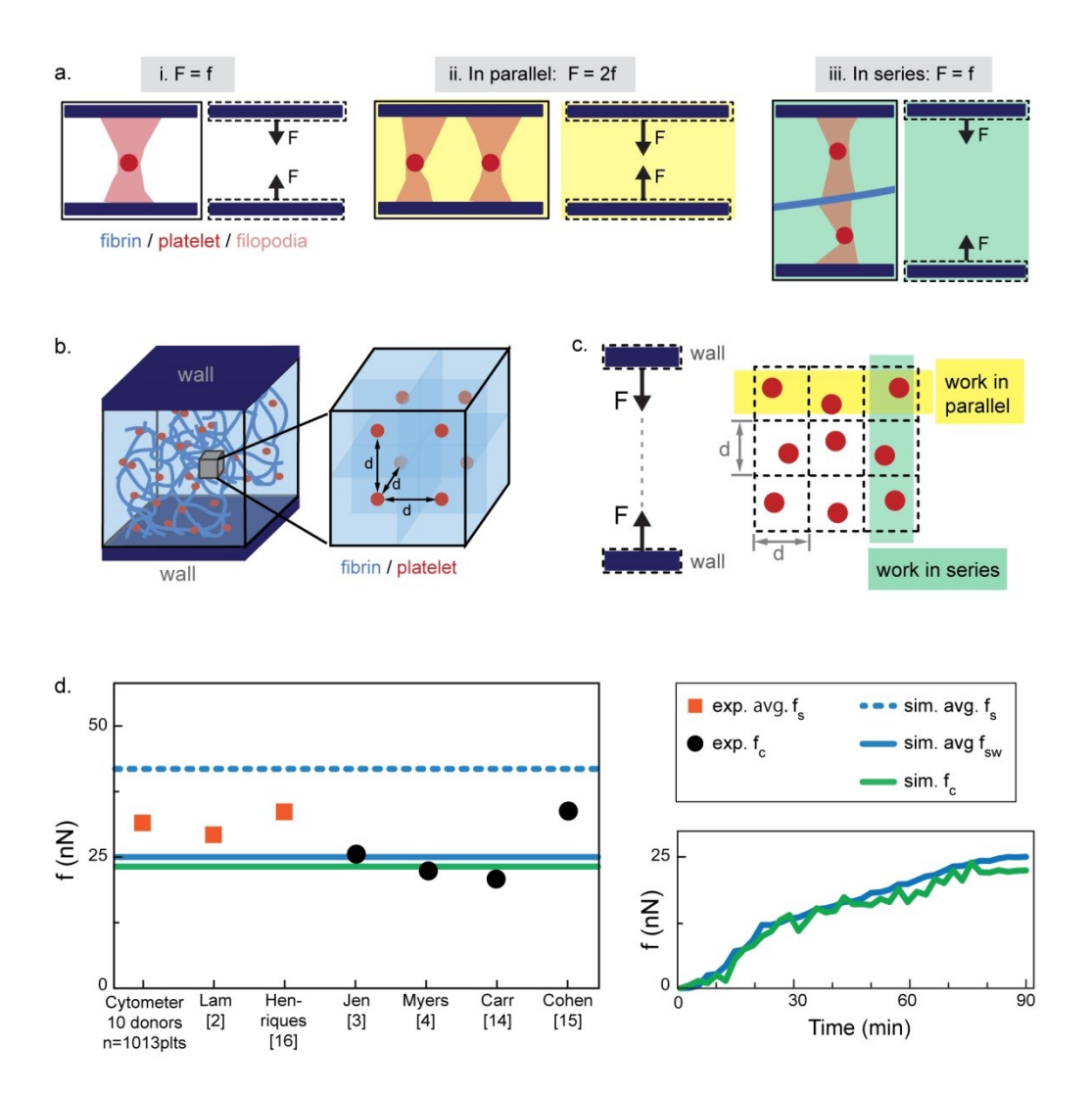


Figure 3: (a) Different arrangements of platelets between two parallel walls affect the overall force applied to the walls. A platelet (in red) contracting between two walls (i) applies a total force f. Two platelets arranged in parallel (ii) apply a total force 2f while two platelets arranged in series (iii) apply a total force f. (b) When platelets are distributed uniformly inside the clot, the distance between two adjacent platelets is f. (c) With such uniform distribution, platelets aligned in the direction of the walls contract together in parallel, and platelets aligned in the direction normal to the walls contract together in series. (d) Single platelet forces evaluated using different methods: squares denote the average of f measured in the experiments, circles denote f calculated from clot force measured in the experiments, doted blue line denotes the average of f in the simulations, solid blue line denotes the average of f in the simulations.

directions, whereas clot force is normal to the wall. Thus, f_c can somewhat underestimate the average of f_s depending on the clot boundary conditions. In our simulations, we can account for the difference between f_c and the average of f_s by only including the force component that is directed towards the wall when evaluating f_s . Indeed, the average of single platelet force normal to the wall f_{sw} shows close agreement with f_c (Figure 3d and Supplementary Figure 4).

Platelet count per unit volume n and fibrin cross-link concentration c vary as nascent clots form under different conditions that can lead to healthy and abnormal clots [37]. We therefore examine the contraction of clots with a wide range of platelet counts $20 \times 10^6 < n < 2000 \times 10^6$ plt/mL (Figure 4a). Note that $n < 150 \times 10^6$ plt/mL is considered as the low platelet count, whereas $n > 450 \times 10^6$ plt/mL is considered as the high platelet count. For each n we alter the fibrin cross-link concentration c which leads to varying fibrin mesh density, to probe the effect of fibrin mesh properties on clot contraction (Figure 4b).

We find that clot force is mainly determined by n, with clots containing more platelets apply greater forces at the end of the contraction period. Fibrin cross-link concentration affects clot force to a lesser extent, leading to a slightly larger F for increased c (Figure 4c). On the other hand, the single platelet forces within the clot f_{sw} is practically constant at the high platelet count range and rapidly drops with n decreasing below 150×10^6 plt/mL (Figure 4d). In the high platelet count range, we find that platelets apply f_{sw} with similar magnitudes independent of c. At the same time, the clot force F is greater for higher c, indicating that an increased cross-link concentration facilitates more efficient force transmission within the clot (Figure 4d). For the entire range of platelet concentrations, f_c is in close agreement with f_{sw} , with minor deviations due to dependence of clot force on fibrin cross-link concentration.

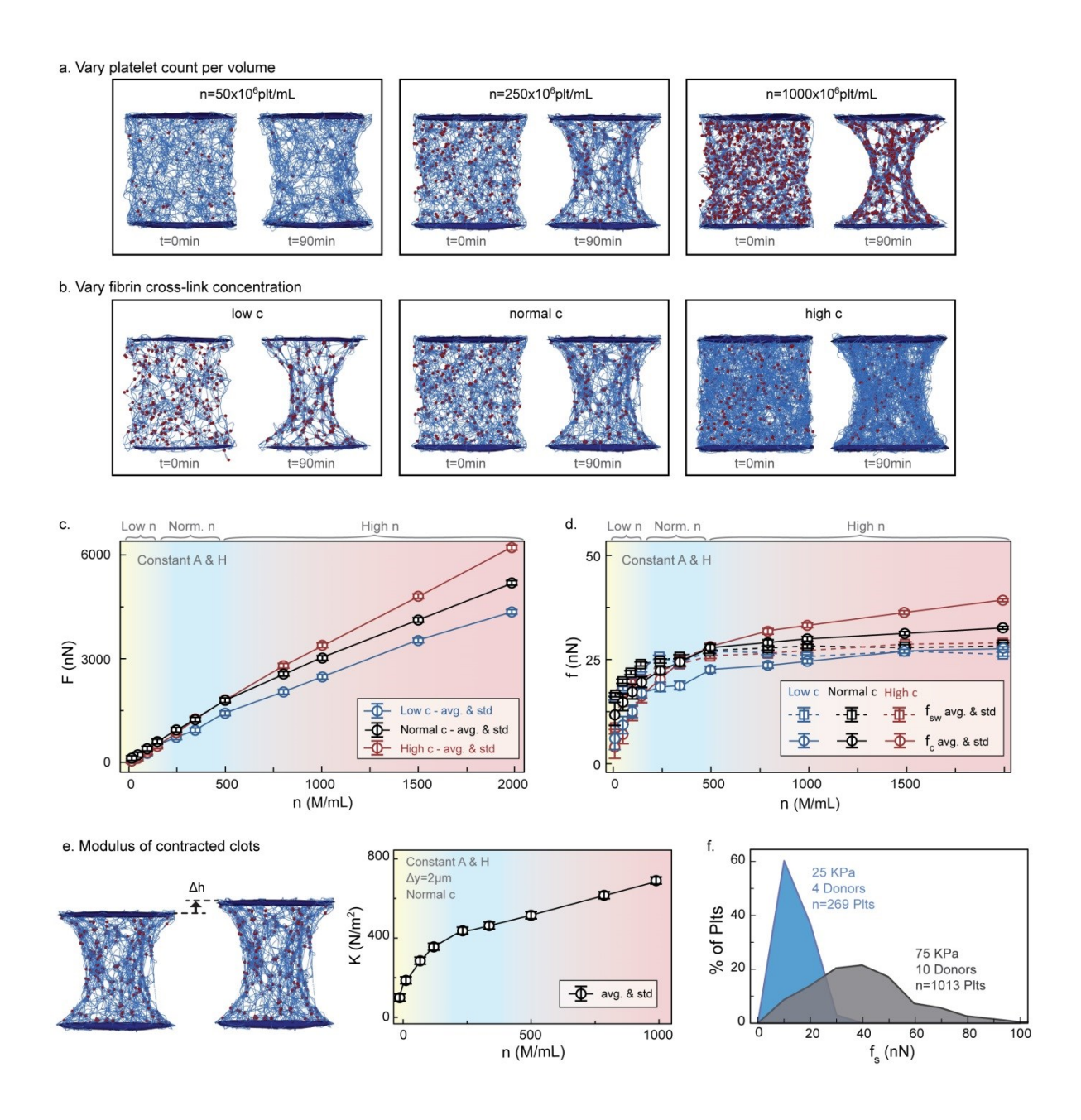


Figure 4: (a) The initial and final states of platelet fibrin clots with varying n contracting between two rigid walls. The clots have constant V, c, cross-section geometry. (b) The initial and final states of platelet fibrin clots with varying c. The clots have constant V, n, cross-section geometry. In (a) and (b), platelets are shown in red, fibrin fibers are in blue, and walls are in dark blue. (c) Clot force F applied on the walls at t = 90 min increases when the clot is populated with more platelets or contains more fibrin corsslinks. (d) Single platelet forces at t = 90 min for clots with varying n and c. (e) Once a clot is fully contracted in simulation, we apply additional force ΔF on the walls to increase the height of the clot by a small Δh . We calculate bulk mudulus as $K = V(\Delta F/A)/\Delta V$. (f) Experimentally measured single platelet forces with our microfabricated contraction cytometer depend on the substrate stiffness.

Remarkably, we also find that our model recapitulates platelet mechanosensing, where platelets modulate force depending on the mechanical microenvironment. In our model, contracted clots with low platelet counts have a significantly lower bulk modulus (Figure 4e). As such the platelets within the clot

experience a less stiff environment leading to a decrease in the ability of the platelets to generate force (Figure 4d and 4e). We can relate this decrease in f_{sw} at low platelet counts to the inability of platelets to generate significant contractile forces in clots with a large amount of loose fibers that do not provide sufficient resistance to the filopodia retraction. In very soft clots, our model shows that the mean platelet force is approximately half the force seen in stiffer clots, and is in agreement with our contraction cytometer data. As the basic unit of our microfabricated contraction cytometer is a platelet pulling on two fibrin(ogen) dots that are covalently cross-linked to a polyacrylamide hydrogel, changing the microenvironmental stiffness experienced by single platelets can be achieved with a straightforward modification of the ratio of acrylamide to bis-acrylamide in the hydrogel [5]. Our calculations [5] show that 25 kPa gels recapitulate conditions associated with soft, loose fibrin networks, whereas 75 kPa gels recapitulate conditions associated with higher stiffness clots. To that end, our data shows that the average single platelet force on 25 kPa gels is approximately half of that of 75 kPa gels (Figure 4f).

To apply force on the walls, a contracting clot needs to bind the fibrin at the outer clot surfaces to the wall. Fibrin readily adsorbs on bare wall surfaces. Thus, we assume that a layer of fibrin is present on the walls to facilitate the clot-wall attachment. To investigate the effect of clot-wall attachment on the clot and platelet forces, we vary the number of connection points between the clot fibrin and the wall, noted as N_a . For attaching fibrin to the wall, we use N_f potential connection points within a volume defined by a small distance δ_0 away from the wall. The value of N_f is determined by the fibrin cross-link concentration c and is sufficient to have all fibers at the clot boundary attached to the wall. We examine different values of N_a in the range $0 \le N_a/N_f \le 1$ corresponding to varying clot-wall attachment conditions (Figure 5a). Here, $N_a = 0$ represents a free clot that is not attached to the walls. Our results show that clot force drops significantly when the clot is poorly attached to the walls (Figure 5b). Interestingly, the force f_{sw} generated by the platelets is nearly insensitive to the attachment conditions as long as there is even a small number of connection points between the clot and the walls (Figure 5c). In the free clot situation, the net force generated by the clot is zero. Still the platelets within the clot generate a substantial force f_{sw} to

deform the fibrin network and to maintain it in the contracted state. We find that f_{sw} can be successfully predicted using the clot force as $f_c = F/(n^{2/3}A)$ when $N_a/N_f \gtrsim 0.25$, and that f_c somewhat underestimates f_{sw} when the clot is poorly attached to the walls (Figure 5c). Note that for $N_a/N_f < 0.25$, the clot-wall attachment is incomplete with multiple fibers at the boundary untethered, which alters the force distribution within the contracting clot and effectively reduces its cross-sectional area (Figure 5a).

a. Altered clot-wall attachment conditions

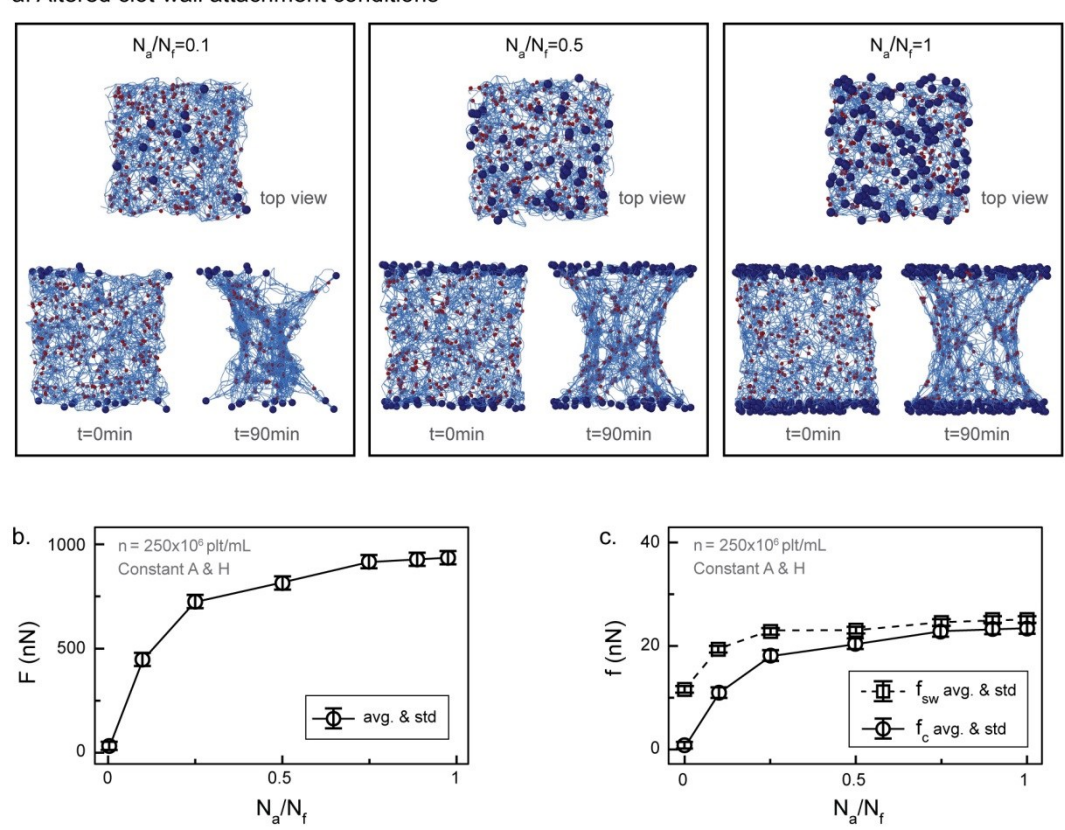


Figure 5: (a) Clot-wall attachment affects clot contraction between walls. The clots have identical V, $n=250\times 10^6$ plt/mL, c, and cross-section geometry. Each dot in dark blue indicates a clot attachment point. Simulated platelets are in red, fibrin fibers are in blue, and wall beads are in dark blue. (b) Clot force F applied on the walls at t=90 min depends on how well the clot is attached to the walls. (c) Single platelet force generated by platelets f_{sw} is nearly constant when the clot has sufficient attachment to the walls. When the clot is free, platelets generate lower forces. When the clot is poorly attached to the walls, it affects the clot internal homogeneity, resulting in deviation of f_c from f_{sw} .

Nascent clots can form with different shapes [36] due to the geometric constraints in the blood vessel, and the influence of the hemodynamic and external forces [38]. We further examine forces generated by clots contracting between tilted and non-flat walls, representing varying blood vessel geometry

constraints. In these simulations, we keep constant the clot volume V, platelet count n, and fibrin cross-link concentration c, and only vary the wall geometry. In the case of tilted walls, the walls are rotated at an angle θ from the midplane (Figure 6a), whereas for non-flat walls, the walls have a constant curvature R (Figure 6b). In all the cases, the initial cross-sectional area of the clots remains the same. We find that the resulted clot force is not affected by θ and R (Figure 6c and 6d). Thus, the simulations indicate that the wall geometry has a minor influence on the net clot force. This is consistent with our conclusion that the clot force is defined by the clot cross-sectional area and therefore the number of platelets that apply the force in parallel. We also find that the forces generated by individual platelets f_{sw} are insensitive to the wall geometry and can be successfully predicted using the clot force as $f_c = F/(n^{2/3}A)$ (Figure 6e and 6f). Note that in this case the area A is the cross-sectional area of the clot normal to the direction connecting the centroids of the opposing wall surfaces.

In figure 7, we probe the force generated by clots with varying cross-sectional area. Specifically, we consider clots with trapezoidal geometry where the clot cross-sectional area at the top wall A_1 is smaller than the clot cross-sectional area at the bottom wall A_2 (Figure 7a). We change the ratio A_1/A_2 by simultaneously decreasing A_1 and increasing A_2 such that the clot volume V and height H remain constant, i.e. $A_1 + A_2 = \text{const.}$ We find that clot force F and single platelet force f_{sw} slightly decrease with decreasing A_1/A_2 (Figure 7b, 7c). Furthermore, the single platelet force $f_c = F/(n^{2/3}A)$ with A being the average clot cross-section area of the clot matches closely to the average f_{sw} of individual platelets within the clot (Figure 7c). These results suggest that a clot generates the maximum contracting force when its initial cross-sectional area is uniform. When $A_1 < A_2$, the clot can be represented by section I which is connected to both walls and two sections II that are only connected to the bottom wall as illustrated in figure 7d. We relate the reduction in the clot force to the fact that sections II are unable to directly impose force on the top wall thereby reducing the net force generated by the clot. This also results in the reduction of the mean forces of the individual platelets in trapezoidal clots.

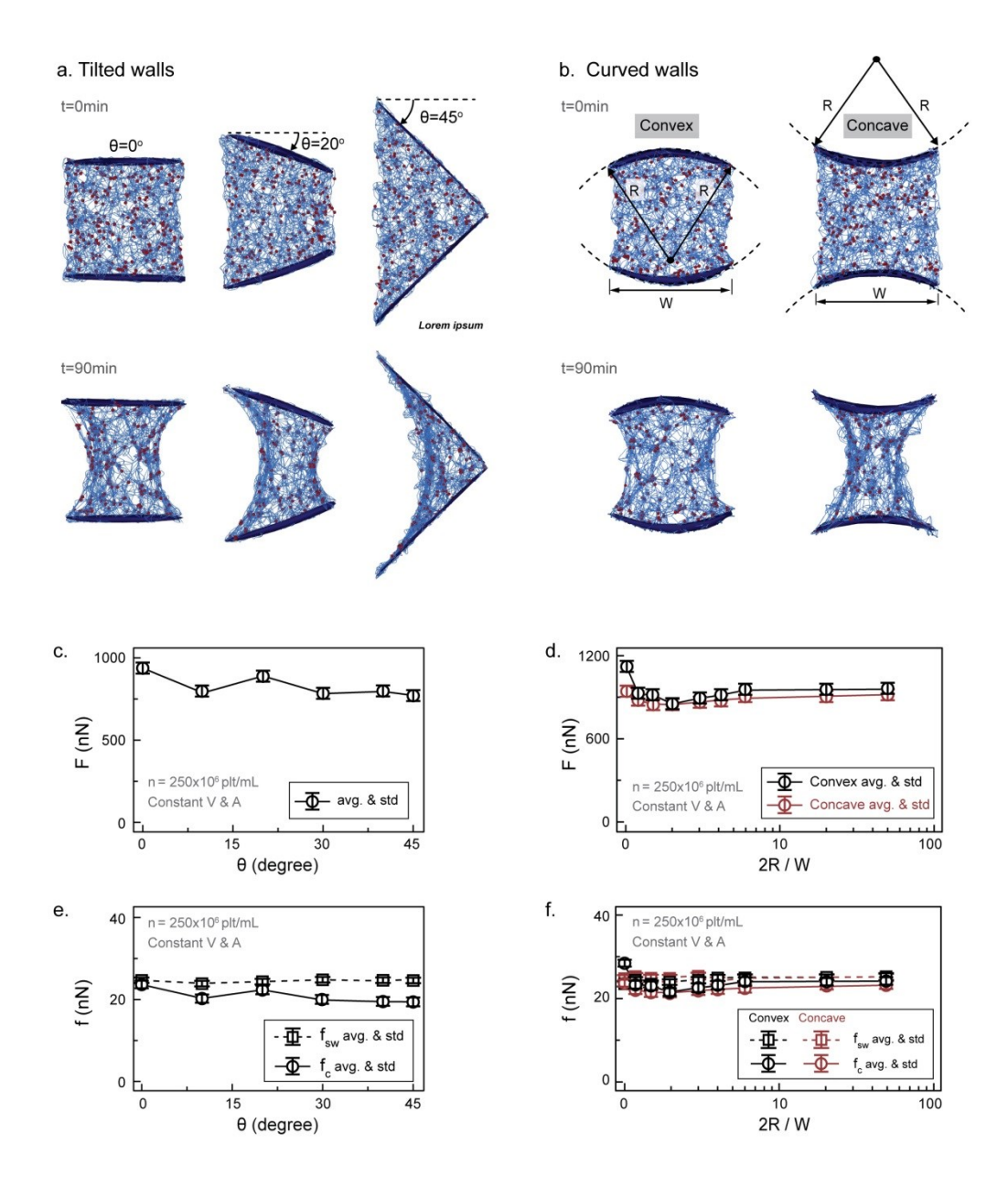


Figure 6: (a) The initial and final states of platelet-fibrin clots contracting between two tilted walls with varying angle θ . (b) The initial and final states of platelet-fibrin clots contracting between two curved walls (convex and concave) with varying curvature R. The clots in (a) and (b) all have constant V, n, c, and cross-sectional area A of the clot normal to the direction connecting the centroids of the two walls. Platelets are shown in red and fibrin fibers are shown in blue. Panels (c) and (d) show clot force F at t = 90 min. Panels (e) and (f) show single platelet force in the direction of walls f_{sw} and the estimated f_c calculated based on the clot force.

a. Clots with cross-section area which varies at different heights

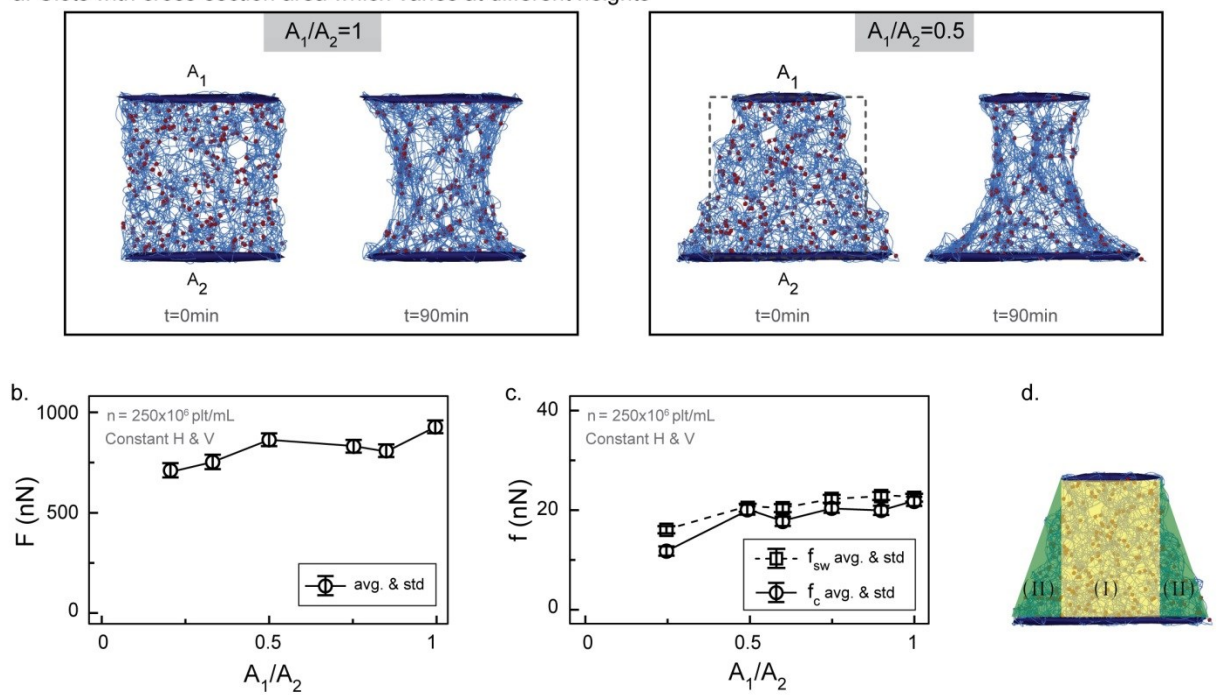


Figure 7: (a) The initial and final states of platelet fibrin clots between two parallel walls with different areas. The cross-sectional area of each clot varies linearly from one wall to the other. The clots have constant V, H, n and c. Platelets are shown in red, fibrin fibers are in blue, and walls are in dark blue. (b) Clot force F slightly increases as the ratio of A1/A2 increases towards unity. (c) Average single platelet forces slightly increases with increasing A1/A2. Here, f_{sw} is obtained in the simulatoins by averaging forces of individual platelets and f_c is calculated based on the clot force at t=90 min. (d).The clot geometry can be represented by two regions I and II with different attachment to the walls.

CONCLUSIONS

In an attached clot, individual platelet activities apply forces contracting nearby fibrin fibers generating the clot force and changing the clot structure and mechanical properties. We utilize an experimentally informed and validated mesoscale computational approach to model platelet-fibrin clot contracting between two rigid walls. The single platelet dynamics is specified based on the experimental measurements of individual platelets and platelet activation patterns within the clot, whereas the fibrin mesh is constructed based on the digitization of an experimental platelet-fibrin clot [36]. The model provides a unique opportunity to probe bulk clot forces, clot structural changes, and to monitor platelet forces at the level of individual filopodia during the clot contraction. We employ this model to explain how local forces of individual platelets are applied to the constraining walls through the elastic fibrin

we find that the mechanical stress within the clot is independent of the clot size and aspect ratio and is mostly defined by the platelet concentration and fibrin density. The clot force is mainly determined by the clot cross sectional area, whereas the clot height and shape have minor effect. This result suggests that the number of platelets in the clot cross section defines the total clot force. We estimate this number and derive a relationship between the single platelet force and the net clot force. By comparing the platelet and clot forces with experimental measurements, we show that our model correctly estimates the single platelet force from the clot forces, and even recapitulates platelet mechanosensing behavior. Furthermore, the model can be used to predict the net clot force based on the platelet and clot properties. We validate that our correlation is applicable to clots with varying platelet count, fibrin cross-link concentration, wall-fibrin attachment condition, and wall geometries, thus capable of predicting the clot contraction forces for a wide range of physiologically relevant conditions. More importantly, our model provides a highly needed link between the individual platelet force measurements and bulk clot force measurements in different experiments revealing that in these previous experiments the forces on the single platelet level are roughly identical.

Our work contributes to better understanding of single platelet function, showing that platelets are able to sense and react to their surrounding microenvironment. In our model, single platelets have the ability to exert same amount of maximum force, and the force can be applied to all directions with no preference. We notice that while platelets are contracting within fibrin scaffolds, they tend to apply larger amount of force in the directions towards the bounding walls compared to the other directions. This is due to the fact that platelet force is related to the resistance from the local fibrin fibers. This also explains why platelets exert lower forces in the clots with low platelet counts or poor wall-fibrin attachment conditions. In these cases, multiple fibrin fibers remain unstressed and can be pulled by the platelets with lower forces. Hence, our model recapitulates the phenomenon of platelet mechanosensing, seen previously [3, 5] as well as in our experiments with the highest number of single platelet measurements reported to date.

Our work establishes the correlation between the microscale cell biophysical properties and the macroscale behavior of the biological material, revealing the mechanism by which individual platelets arrange within blood clots to yield the clot force. The results of our work allow one to predict the final clot force and clot structure based on the known single platelet properties. Furthermore, our results indicate how the measured clot force can be used as an indicator of single platelet force. This could assist the develop of new clinical diagnostic techniques that utilize bulk clot force measurements as indicators of different platelet deficiencies. Our findings can also be applied to contracting cells that are embedded in and contract against a scaffold beyond platelets, such as myofibroblasts, and even semisynthetic and synthetic platelets mimics. Finally, our model can facilitate the design, application, and optimization of grafts for treating wounds, composed of PRP, PRF, and platelet-inspired biomaterials. In particular our model can be useful for the engineering of platelet-based biomaterials and biomaterials with synthetic platelets with specific geometry to precisely fit the wound site to achieve the desired levels of stress and stiffness for the enhanced efficacy.

Limitation of the study

While our model captures the basic mechanism of platelet-driven clot contraction, it has limitations that can be addressed in future work. Our model does not consider platelet adhesion to the vessel wall via collagen or von Willebrand factor, although these are typical interactions occurring during the initial phase of hemostasis. Our model does not incorporate the effects of fluid flow, shear stress, and red blood cells on the clot contraction process. The size of the clot we model is relatively small limited the by computational resources. Thus, the model predictions may be less accurate for large scale clots. Although our mesoscale model does not include all the factors relevant to biological clots, it is able to successfully capture the clot contraction process under physiological conditions [36]. Furthermore, this approach can be further expanded to model the activity of additional cell types in biological materials.

Our model is built and validated with the platelet dynamics and bulk clot contraction process under physiological conditions of pH, salt, and temperature, allowing us to examine the mechanics of the generation of clot force, the effect of platelet concentration, fibrin network density, and clot-wall attachment on the contraction process. Note that we cannot directly examine how the clot contraction process changes due to variations in pH, salt, and temperature conditions.

STAR * METHODS

Detailed methods are provided in the online version of this paper and include the following:

- KEY RESOURCES TABLE
- RESOURCE AVAILABILITY
 - Lead contact
 - o Materials availability
 - o Data and code availability

• METHOD DETAILS

- o Computational model of platelet-fibrin clot contracting between walls
- Fibrin mesh
- o Platelets
- o Clot-wall attachment
- Bulk clot force
- Single platelet force
- Clot contraction between flat parallel walls
- Clot contraction between tilted and non-flat walls

ACKNOWLEDGEMENTS

Financial support provided by NIH R35 (HL145000) to WAL; NIH R21 (EB026591), NIH K25 (HL141636), & NIH R01 (HL155330) to DRM, NSF 1809566 to WAL and DRM, NIH F31 (HL160210-

01) and American Society of Hematology Minority Medical Student Award Program Fellowship to OO and NSF 1809227 to AA. The work used the Extreme Science and Engineering Discovery Environment (XSEDE) provided through Award TG-DMR180038.

AUTHOR CONTRIBUTIONS

Y.S., D.R.M., W.A.L., and A.A. planned the work. Y.S. developed the computational model and carried out the simulations. O.O. and D.R.M. carried out the experiments. Y.S., D.R.M., W.A.L., and A.A. interpreted the data and wrote the manuscript.

DECLARATION OF INTEREST

The authors declare no competing interests.

REFERENCES

- 1. Cines, D.B., et al., *Clot contraction: compression of erythrocytes into tightly packed polyhedra and redistribution of platelets and fibrin.* Blood, 2013. **123**(10): p. 1596-1603.
- 2. Kim, O.V., et al., *Quantitative structural mechanobiology of platelet-driven blood clot contraction.*Nat. Commun, 2017. **8**(1): p. 1274.
- 3. Lam, W., et al., *Mechanics and contraction dynamics of single platelets and implications for clot stiffening.* Nature materials, 2011. **10**(1): p. 61-66.
- 4. Jen, C.J. and L.V. McIntire, *The structural properties and contractile force of a clot.* Cell Motil., 1982. **2**(5): p. 445-455.
- 5. Myers, D.R., et al., *Single-platelet nanomechanics measured by high-throughput cytometry.* Nature materials, 2017. **16**(2): p. 230-235.
- 6. Krishnaswami, A., et al., *Patients with coronary artery disease who present with chest pain have significantly elevated platelet contractile force and clot elastic modulus.* Thromb Haemost 2002. **88**(05): p. 739–744.
- 7. Williams, E.K., et al., Feeling the Force: Measurements of Platelet Contraction and Their Diagnostic Implications. Seminars in Thrombosis and Hemostasis, 2019. **45**(3): p. 285-296.
- 8. Carr, M.E., Development of platelet contractile force as a research and clinical measure of platelet function. Cell biochemistry and biophysics, 2003. **38**(1): p. 55-78.
- 9. Tomasiak-Lozowska, M.M., et al., *Reduced clot retraction rate and altered platelet energy production in patients with asthma*. J Asthma 2016. **53(06)**: p. 589–598.
- 10. Greilich, P., et al., *Quantitative assessment of platelet function and clot structure in patients with severe coronary artery disease.* Am J Med Sci 1994. **307(01)**: p. 15–20.
- 11. Tomasiak-Lozowska, M.M., et al., *Asthma is associated with reduced fibrinolytic activity, abnormal clot architecture, and decreased clot retraction rate.* Allergy, 2017. **72(02)**: p. 314–319.

- 12. Misztal, T., Rusak, T., and Tomasiak, M.,, *Peroxynitrite may affect clot retraction in human blood through the inhibition of platelet mitochondrial energy production.* Thromb Res 2014. **133(03)**: p. 402–411.
- 13. Le Minh, G., et al., *Impaired contraction of blood clots as a novel prothrombotic mechanism in systemic lupus erythematosus.* Clin Sci (Lond) 2018. **132**(02): p. 243–254.
- 14. White, N.J., et al., *Clot formationis associated with fibrinogen and platelet forces in a cohort of severely injured emergency department trauma patients.* Shock, 2015. **44**(Suppl 1): p. 39–44.
- 15. Henriques, S.S., et al., *Force field evolution during human blood platelet activation.* J. Cell Sci, 2012. **125**(16): p. 3914–3920
- 16. Carr, M.E. and S.L. Zekert, *Measurement of Platelet-Mediated Force Development During Plasma Clot Formation.* Am J Med Sci, 1991. **302**(1): p. 13-18.
- 17. Cohen, I., and De Vries, A., *Platelet contractile regulation in an isometric system.* Nature, 1973. **246**(5427): p. 36-37.
- 18. Drew, A.F., et al., *Wound-healing defects in mice lacking fibrinogen.* Blood, 2001. **97**(12): p. 3691–3698.
- 19. Clark, R.A., et al., *Transient functional expression of alphaVbeta 3 on vascular cells during wound repair.* Am J Pathol, 1996. **148**(5): p. 1407-1421.
- 20. Knighton D.R., et al., Classification and treatment of chronic nonhealing wounds. Successful treatment with autologous platelet-derived wound healing factors (PDWHF). Ann Surg, 1986. **204**(3): p. 322-330.
- 21. Arora, S. and N. Agnihotri, *Platelet Derived Biomaterials for Therapeutic Use: Review of Technical Aspects.* Indian J Hematol Blood Transfus, 2017. **33**(2): p. 159-167.
- 22. *Platelet-Rich Fibrin and Soft Tissue Wound Healing: A Systematic Review.* Tissue Engineering Part B: Reviews, 2017. **23**(1): p. 83-99.
- 23. Textor, J., Platelet-Rich Plasma (PRP) as a Therapeutic Agent: Platelet Biology, Growth Factors and a Review of the Literature, in Platelet-Rich Plasma: Regenerative Medicine: Sports Medicine, Orthopedic, and Recovery of Musculoskeletal Injuries, J.F.S.D. Lana, et al., Editors. 2014, Springer Berlin Heidelberg: Berlin, Heidelberg. p. 61-94.
- 24. Marx, R.E., et al., *Platelet-rich plasma: Growth factor enhancement for bone grafts*. Oral surgery, oral medicine, oral pathology, oral radiology, and endodontics, 1998. **85**(6): p. 638-646.
- 25. Bernasek, T.L., et al., Effect on Blood Loss and Cost-Effectiveness of Pain Cocktails, Platelet-Rich Plasma, or Fibrin Sealant After Total Knee Arthroplasty. The Journal of Arthroplasty, 2012. 27(8): p. 1448-1451.
- 26. Nanditha, S., et al., *Apprising the diverse facets of Platelet rich fibrin in surgery through a systematic review.* International Journal of Surgery, 2017. **46**: p. 186-194.
- 27. O'Connell, S.M., et al., *Autologous platelet-rich fibrin matrix as cell therapy in the healing of chronic lower-extremity ulcers.* Wound Repair Regen, 2008. **16**(6): p. 749-56.
- 28. Kuffler, D.P., et al., *Neurological recovery across a 12-cm-long ulnar nerve gap repaired 3.25 years post trauma: case report.* Neurosurgery, 2011. **69**(6): p. E1321-6.
- 29. Tse, J.R. and A.J. Engler, *Stiffness gradients mimicking in vivo tissue variation regulate mesenchymal stem cell fate.* PLoS One, 2011. **6**(1): p. e15978.
- 30. Engler, A.J., et al., *Matrix elasticity directs stem cell lineage specification*. Cell, 2006. **126**(4): p. 677-89.
- 31. Burnouf, T., et al., *Blood-derived biomaterials: fibrin sealant, platelet gel and platelet fibrin glue.* ISBT Science Series, 2009. **4**(1): p. 136-142.
- 32. Sekhon, U.D.S. and A.S. Gupta, *Platelets and Platelet-Inspired Biomaterials Technologies in Wound Healing Applications.* ACS Biomater. Sci. Eng., 2017. **4**(4): p. 1176-1192.

- 33. Oshinowo, O., et al., Significant differences in single-platelet biophysics exist across species but attenuate during clot formation. Blood Adv, 2021. **5**(2): p. 432-437.
- 34. Carr, M.E., Jr. Krischnaswami, A. and Martin, E., *Method of using platelet contractile force and whole blood clot elastic modulus as clinical markers.* US Patent 2007. **7,192,726**.
- 35. Qiu, Y., et al., *Platelet mechanosensing of substrate stiffness during clot formation mediates adhesion, spreading, and activation.* Proceedings of the National Academy of Sciences of the United States of America, 2014. **111**(40): p. 14430-14435.
- 36. Sun Y., et al., *Platelet heterogeneity enhances blood clot volumetric contraction: An example of asynchrono-mechanical amplification.* Biomaterials, 2021. **274**.
- 37. Tutwiler, V., et al., *Kinetics and mechanics of clot contraction are governed by the molecular and cellular composition of the blood.* Blood, 2016. **127**(1): p. 149-159.
- 38. Jackson, S.P., *The growing complexity of platelet aggregation*. Blood, 2007. **109**(12): p. 5087-95.